J. Synchrotron Rad. (1996). **3**, 207–212

Phase Shift and Radiation Spectrum of a Straight Series of Undulators

Y. Miyahara

SPring-8, Kamigori, Ako-gun, Hyogo 678-12, Japan

(*Received 10 May 1996; accepted 23 May 1996*)

In constructing a very long undulator it is convenient to separate the undulator into a number of sections with a constant gap distance between the sections. The properties of the radiation spectrum expected in such an undulator were investigated assuming ideal short undulators for each section. It is shown that the peak height and width of the spectrum do not deteriorate if the radiation phases of the sections are matched to each other, even with a large gap distance. This can be realized by adjusting the field strength of the three-pole wigglers installed in each gap.

Keywords: long undulators; separated sections; phase shift; radiation spectrum.

1. Introduction

The brilliance of synchrotron radiation in storage rings has been increased by reducing the emittance of the electron beam to several nm rad and by installing undulators several metres long. Higher brilliance can be obtained by increasing the undulator length, while it is partly limited by the degree of the emittance. In the storage ring of SPring-8, for instance, a 30 m-long undulator can be installed in a long straight section, which is made available by rearranging quadrupole magnets in the storage ring (Hara *et al.*, 1990). A very long undulator is also required for a single-pass free-electron laser in storage rings and linacs. In constructing such a long undulator it is convenient to separate the undulator into a number of short sections. This method has been applied to undulators several metres long at the ESRF (Chavanne *et al.*, 1992), ELETTRA (Diviacco & Walker, 1993) and KEK-MR (Yamamoto, Shioya, Kitamura & Tsuchiya, 1995).

In these cases each section is tightly connected to avoid deterioration of the radiation spectrum. There then arises the question of to what extent the gap distance between the sections can be lengthened without deteriorating the spectrum. Furthermore, in some cases it might be useful to install steering magnets between the sections for correcting the beam axis, or to install quadrupole magnets for reducing the electron beam size. Thus, the gap distance might be in the range 0.1–200 mm depending on the requirements and limitations in constructing the undulator.

The gap distance induces a phase shift between the radiation generated in different sections, which affects the radiation spectrum of the undulator. This problem has been studied in detail in the case of two sections or the optical klystron (Elleaume, 1983). In the present paper we investigate the effects in the case of a long undulator separated into many sections. For simplicity we regard each section as an ideal undulator. We discuss numerical examples of a 30 m-long undulator for SPring-8, which is tentatively assumed to be separated into ten sections to generate X-rays.

2. Radiation spectrum

2.1. *Phase shift*

The radiation wavelength of the nth harmonic of a planar undulator is given by

$$\lambda_n = (\lambda_0/2n\gamma^2)[1 + K^2/2 + (\gamma\theta)^2] , \qquad (1)$$

where λ_0 is the undulator period, γ is the Lorentz factor, K is the K parameter and θ is the radiation angle from the beam axis. This expression can be obtained from the following relation:

$$(\lambda_0 + n\lambda_n)/c = \lambda_0/c\beta_z \cos\theta, \qquad (2)$$

with $\beta_z = \beta(1 - K^2/4\gamma^2)$ and $\beta = (1 - 1/\gamma^2)^{1/2}$, where $c\beta_z \cos\theta$ is the average electron velocity component in the θ direction. Equation (2) implies that the nth harmonic wave proceeds by n periods in front of the electron when the electron travels over one period λ_0. Accordingly, an electron passing through an undulator of N_u period generates an nth harmonic wave with nN_u periods in front of the electron at the exit of the undulator.

Now we consider the nth harmonic wave on the beam axis, generated by an electron passing through a series of undulators as shown in Fig. 1, where the pulsed waves $W1$ and $W2$, with length τ in time, schematically represent the electric field amplitude. The transit time of the electron and wave over a gap distance L_d between the undulators follows the relation:

$$(L_d + c\Delta t)/c = L_d/c\beta. \qquad (3)$$

Here, Δt represents the transit-time difference between the

electron and wave over the gap distance L_d. Thus, we obtain

$$\Delta t = (L_d/c)(1/\beta - 1) \simeq (L_d/c)/2\gamma^2. \quad (4)$$

Note that Δt is markedly reduced by the factor $1/2\gamma^2$ compared with the transit time L_d/c of the light. In the case of a series of M undulators separated by a constant gap distance, we have a pulse train of waves of length τ, as shown at the bottom of Fig. 1.

The phase difference between the first and mth pulse waves is

$$\Delta\varphi = 2\pi(m - 1)\Delta t/\tau_n \simeq \pi(m - 1)L_d/\lambda_n\gamma^2, \quad (5)$$

where $\tau_n = \lambda_n/c$ is the wavelength in time, while $\tau = nN_u\tau_n$ is the pulse length. For instance, we have $\Delta\varphi = 3.5\pi$ for $m = 10$, $L_d = 10$ mm, $\lambda_n = 0.1$ nm and $\gamma = 16\,000$ or $E = 8$ GeV. Distant pulse waves have a considerably large phase difference. Referring to (1) we have, at $\theta = 0$,

$$\Delta\varphi = [2n\pi/(1 + K^2/2)](m - 1)L_d/\lambda_0. \quad (6)$$

A higher harmonic wave suffers a larger phase shift.

2.2. *Fourier transform*

The radiation spectrum of the pulse wave train of the nth harmonic shown in Fig. 1 can be obtained by the following Fourier transform

$$F(\omega) = (2\pi)^{-1/2} \sum_{m=0}^{M-1} \int_{m(\tau+\Delta t)}^{\tau+m(\tau+\Delta t)} \sin(\omega_n t - \varphi_m)\exp(i\omega t)\,dt = F_0(\omega)G(\omega), \quad (7)$$

where M is the number of pulse waves and $\varphi_m = m\omega_n(\tau + \Delta t)$. Here we have defined

$$F_0(\omega) = (2\pi)^{-1/2} \int_0^\tau \sin(\omega_n t)\exp(i\omega t)\,dt \simeq \left[(\tau/2)(2\pi)^{-1/2}\right][\exp(i\Delta\omega\tau) - 1]/\Delta\omega\tau, \quad (8)$$

$$G(\omega) = \sum_{m=0}^{M-1} \exp[im\omega(\tau + \Delta t)] = 1 + \exp(iMx/2)\sin[(M - 1)x/2]/\sin(x/2), \quad (9)$$

with $\Delta\omega = \omega - \omega_n$ and $x = \omega(\tau + \Delta t)$. Equation (9) is obtained from the following formulae (Moriguchi, Udagawa & Ichimatsu, 1972):

$$\sum_{k=1}^{r} \sin(kx) = \sin[(r + 1)x/2]\sin(rx/2)/\sin(x/2), \quad (10a)$$

$$\sum_{k=1}^{r} \cos(kx) = \cos[(r + 1)x/2]\sin(rx/2)/\sin(x/2). \quad (10b)$$

The intensity of the radiation spectrum is proportional to $|F(\omega)|^2 = |F_0(\omega)|^2|G(\omega)|^2$ with

$$|F_0(\omega)|^2 = (\tau^2/8\pi)[\sin(\Delta\omega\tau/2)/\Delta\omega\tau/2]^2 \quad (11)$$

$$|G(\omega)|^2 = 1 + 2\cos(Mx/2)\sin[(M - 1)x/2]/\sin(x/2) + \{\sin[(M - 1)x/2]/\sin(x/2)\}^2. \quad (12)$$

Note that $|F_0(\omega)|^2$ is the spectrum for one sectional undulator. In the case of $M = 1$ and 2, we have $|G(\omega)|^2 = 1$ and $2(1 + \cos x)$, respectively. The latter agrees with the results from the optical klystron (Elleaume, 1983).

In the same way as in the discussion of the optical klystron, the parameter $x = \omega(\tau + \Delta t)$ in (12) can be expressed as $x = 2\pi N + 2\pi N_d$, with

$$N = nN_u\lambda_n/\lambda \quad (13a)$$

$$N_d = c\Delta t/\lambda \simeq L_d/2\lambda\gamma^2 \quad (13b)$$

for $\lambda = 2\pi c/\omega$. Here, N_d is the number of wavelengths λ in the delay of the electron to the wave when the electron has passed over the gap distance L_d. When a three-pole wiggler is introduced into the gap to lengthen the electron orbit as discussed later, L_d is replaced by the electron orbit length in the gap.

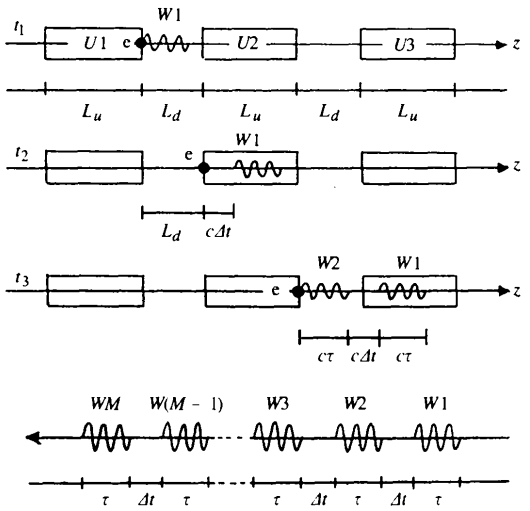

Figure 1
Trajectory of an electron and the pulsed electromagnetic waves generated by the electron passing through a series of undulators.

2.3. *Numerical calculations*

In order to see the properties of the spectrum given by (11) and (12), numerical calculations of the spectrum were performed for the variable ξ (= $\Delta\omega/\omega_n$) with

$$x = 2\pi nN_u(1 + \xi)(1 + \Delta t/\tau), \quad (14a)$$

$$y = \Delta\omega\tau/2 = \pi nN_u\xi. \quad (14b)$$

With the aid of (4) and $\tau = nN_u\lambda_n/c$, the spectrum on the beam axis can be calculated for a given set of parameters M, L_d, N_u, γ, n and λ_n.

Fig. 2 represents an example of the spectrum at M = 2, 5 and 10 for L_d = 0, N_u = 100, n = 1, λ_n = 0.1 nm and E = 8 GeV. This example with L_d = 0 is just for one undulator with a total period MN_u. In Fig. 2 the factor $\tau^2/8\pi$ is not included. We see that the peak height of $|F(\omega)|^2$ is proportional to M^2, and the width to $1/M$, as expected. In the present formalism this is produced by the modulation function $|G(\omega)|^2$, which takes the peak value $|G(x)|^2 = M^2$ periodically at $x = \omega(1 + \Delta t/\tau) = 2\pi k$ (where k is an integer).

Fig. 3 represents the spectrum at different L_d values for the above parameters at M = 10. We see that the peaks of the spectrum $|F(\omega)|^2$ and $|G(\omega)|^2$ shift to the left as L_d increases. Note that the peak height and width of $|G(\omega)|^2$ are independent of L_d. The peak positions y_p of $|G(\omega)|^2$ at different L_d values are shown as solid circles in Fig. 4. We see that the peaks of $|G(\omega)|^2$ and hence $|F(\omega)|^2$ are central (y_p = 0) at L_d = 0, 50, 99, 148 and 198 mm. It is emphasized that in all these cases the peak height and width of the spectrum $|F(\omega)|^2$ are almost the same, which is because $\Delta t/\tau << 1$, as discussed later. We can therefore select the gap distance L_d at these values without deteriorating the quality of the spectrum.

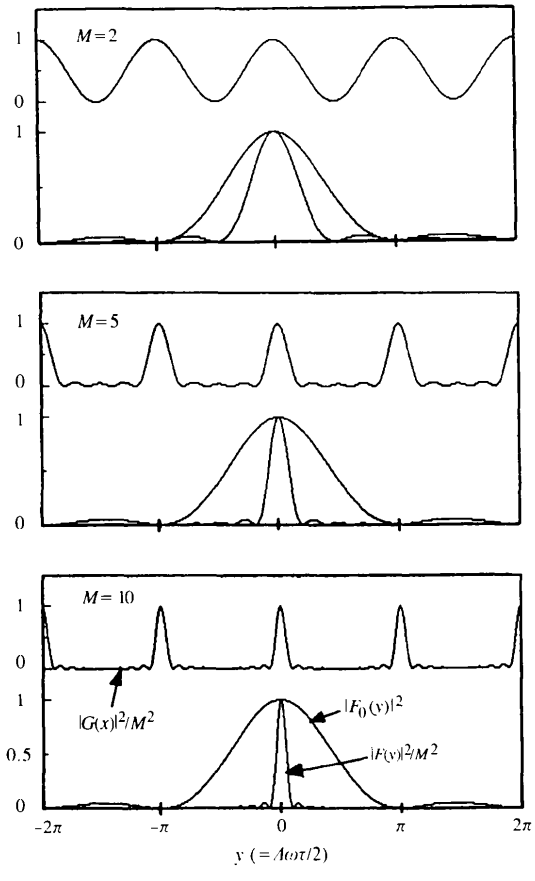

Figure 2
Radiation spectra $|F(\omega)|^2$ and $|F_0(\omega)|^2$ and modulation function $|G(\omega)|^2$ at M = 2, 5 and 10 for L_d = 0, N_u = 100, n = 1, λ_n = 0.1 nm and E = 8 GeV.

The radiation wavelength λ_n can be shifted by changing the undulator field. As indicated in Fig. 4, in which open circles represent λ_n = 0.07 nm and crosses λ_n = 0.13 nm, the peak positions are different depending on the wavelength. The gap distance L_d* at which the peaks come to the centre (y_p = 0) in the above three cases is plotted in Fig. 5 as a function of wavelength. In order to adjust the peak position to the spectrum centre, it is necessary to change the gap distance in accordance with the wavelength. This can be done effectively by introducing a three-pole wiggler between the undulators, like in the optical klystron. Although the purpose of the three-pole wiggler is not to induce electron-energy dispersion but to lengthen the orbit length, we call it the dispersive section after the optical klystron.

Before discussing the dispersive section we consider the relation of the peak position and gap distance shown in Figs. 4 and 5, which can be expressed as

$$L_d\ (\text{mm}) \simeq -(1000/2\pi)\lambda_n(\text{nm})\, y_p + L_d^* \qquad (15a)$$

and

$$L_d^*\ (\text{mm}) \simeq 500h\lambda_n\ (\text{nm}), \qquad (15b)$$

respectively, where h is an integer. These relations can be derived as follows. As mentioned earlier, the modulation function $|G(x)|^2$ is a periodic function, having peaks at x_p = $2\pi k$ (where k is an integer). Therefore, we put

$$2\pi nN_u(1 + \xi_p)(1 + \Delta t/\tau) = 2\pi k. \qquad (16)$$

Since $\Delta t/\tau << 1$ and $y_p = \pi nN_u\xi_p$, we obtain

$$\Delta t \simeq -(\tau/\pi nN_u)y_p + (\tau/nN_u)(k - nN_u). \qquad (17)$$

Using the relations for Δt of equation (4) and τ, we find the following relations:

$$L_d \simeq -(2\gamma^2/\pi)\lambda_n y_p + L_d^*, \qquad (18a)$$

$$L_d^* = 2\gamma^2 h\lambda_n. \qquad (18b)$$

Substituting γ = 16 000, we obtain (15a) and (15b).

In (13b) we have shown that $N_d = L_d/2\lambda_n\gamma^2$ at $\lambda = \lambda_n$. Accordingly, (18a) and (18b) lead to $N_d = -y_p/\pi + h$, so that $N_d = h$ (= integer) when the peak position is at the centre. This implies that integer numbers of the wavelength λ_n exist between the pulse waves in the pulse train shown in Fig. 1. If we substitute L_d* of (18b) for L_d in (5), we get the phase shift $\Delta\varphi = 2h(m - 1)\pi$ between the waves from the first and mth undulators. Under this condition, even with a gap distance, there is no mismatch of the phase, and the peak height of the spectrum is not decreased.

Next we consider the relation of the peak intensity of the spectrum to the gap distance. From (16) we get $\xi_p \simeq -\Delta t/\tau$. Considering the spectrum given in Fig. 3, we find that the

ratio of the peak intensity of the spectrum determined by the undulator series with gap distances and that without gap distances is given by

$$I/I_0 = |F_0(y_p)|^2/|F_0(0)|^2 = |\sin(y_p)/y_p|^2, \quad (19)$$

where $y_p = \pi n N_u \xi_p \simeq -\pi \Delta t/\tau_n = -\pi L_d/2\lambda_n\gamma^2$. In the case of the above example, L_d = 10 mm with λ_n = 0.1 nm, γ = 16 000, we have $y_p = 0.20\pi$, so that the intensity ratio I/I_0 = 0.88.

2.4. *Dispersive section*

The gap distance depends on the requirements and limitations of the undulators to be constructed. As shown in the above example, the reduction of the peak intensity is about 10% or less if the distance is 10 mm or less. In some cases the gap distance needs to be longer. Here we tentatively assume a distance L_d = 80 mm and install a three-pole wiggler made of permanent magnets with a length L_w = 60 mm to adjust the phase mismatch. As shown in the *Appendix*, the transit-time difference between the electron and wave passing through the wiggler section is

$$\Delta t_w \simeq (L_w/c)(1 + 2D)/2\gamma^2, \quad (20)$$

where $D \simeq 3600(B_p L_w)^2$, with B_p the peak field in the wiggler. Then the total transit-time difference over the dispersive section is

$$\Delta t \simeq (L_d/c)(1 + 2DL_w/L_d)/2\gamma^2. \quad (21)$$

For a probable value of B_p = 0–0.3 T, we find (1 + $2DL_w/L_d$) = 1–2.7, so that the effective length of the dispersive section is L_{deff} = 80–220 mm. Accordingly, we can adjust the spectrum peak to the centre (y_p = 0) in the wavelength range λ_n = 0.05–0.15 nm, as indicated by a bold line in Fig. 5.

2.5. *Width of the peak spectrum*

Here, the effects of the emittance and energy spread of the electron beam on the spectrum are briefly considered. As can be seen in Figs. 2 and 3, the peak width of the spectrum is rather narrow and almost determined by the modulation function $|G(x)|^2$. Defining $x = x_p + \Delta x = 2\pi k + \Delta x$, we obtain

$$|G(x)|^2 \simeq M^2 - (1/12)M^2(M^2 - 1)(\Delta x)^2 + O[(\Delta x)^4] \quad (22)$$

so that the half-width is given by

$$\Delta x \simeq [6/(M^2 - 1)]^{1/2} \simeq 6^{1/2}/M. \quad (23)$$

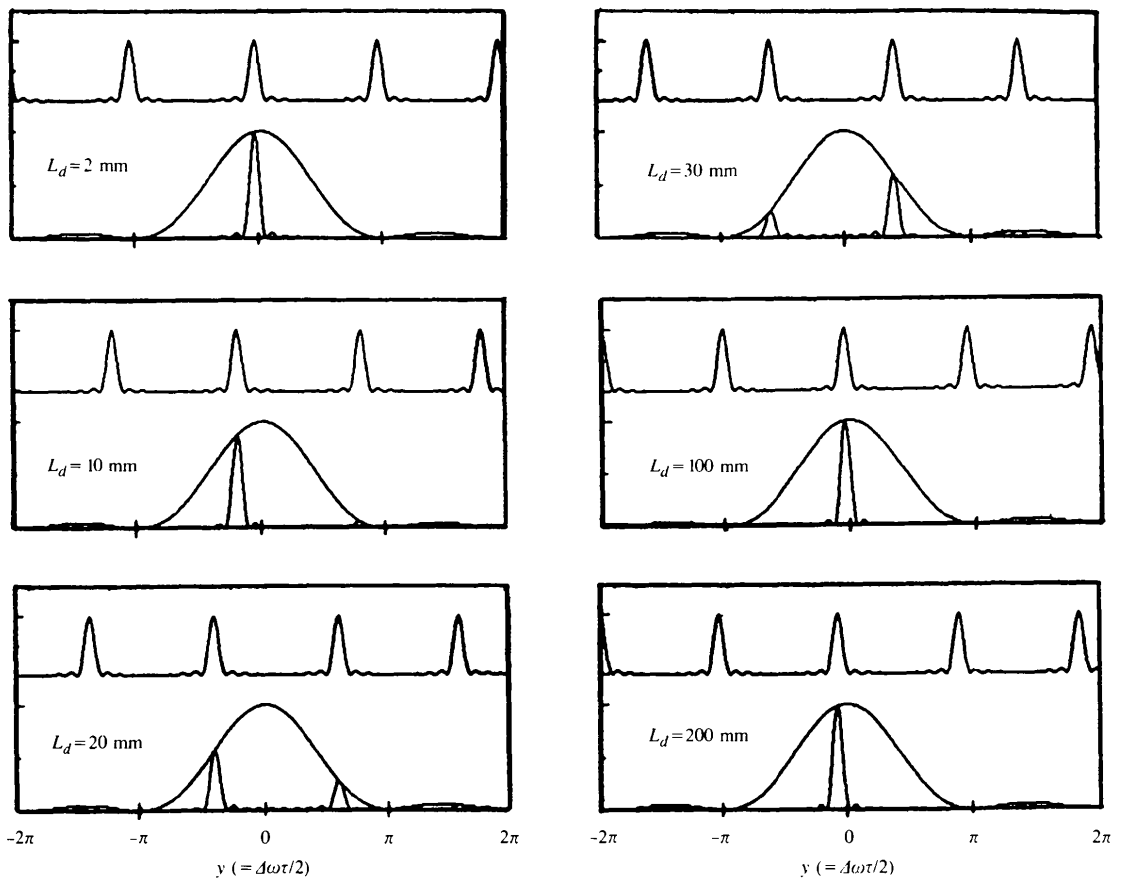

Figure 3
Radiation spectra for N_u = 100, n = 1, λ_n = 0.1 nm, E = 8 GeV and M = 10 at different L_d values. The peak position of the spectra shifts to the left as L_d increases.

Noting the relation $x = \omega(\tau + \Delta t)$, we obtain

$$\Delta\omega/\omega_n \simeq 6^{1/2}/[2\pi n N_u M(1 + \Delta t/\tau)] + 2\Delta\gamma/\gamma - (\gamma\theta)^2/(1 + K^2/2)[1 - L_{\mathrm{deff}}/L_u(1 + K^2/2)]. \quad (24)$$

Owing to the Gaussian distribution of the energy spread (σ_ε/E), the size ($\sigma_{x'}$) and divergence (σ_x) of the electron beam and also of the inclination (σ_θ) of each undulator axis, the peak width of the spectrum is given by the r.m.s. of all terms in (24), with $\langle\theta^4\rangle = \theta_a^4 + \sigma_{x'}^4 + (\sigma_x/L_0)^4 + (\sigma_\theta)^4$, where θ_a is the acceptance angle of the radiation and L_0 is the distance from the undulator to the observation point. A dispersive section reduces the width somewhat by the factor $(1 + \Delta t/\tau)$ in the first term of (24) if $\Delta t/\tau$ is not negligibly small.

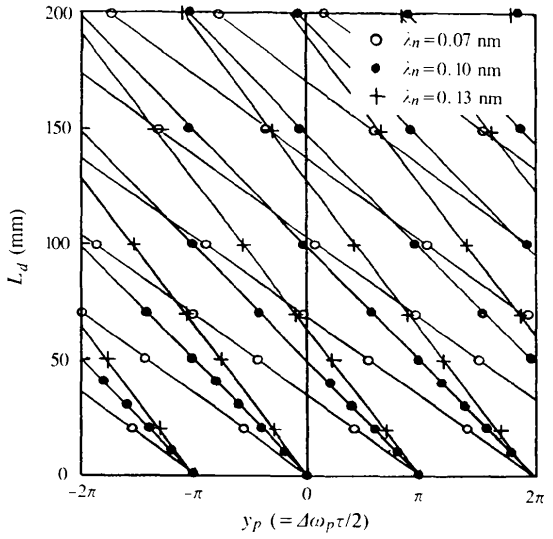

Figure 4
Relation of the peak position y_p of the spectrum at different gap distances L_d for the three cases λ_n = 0.07, 0.1 and 0.13 nm with M = 10, N_u = 100 and E = 8 GeV.

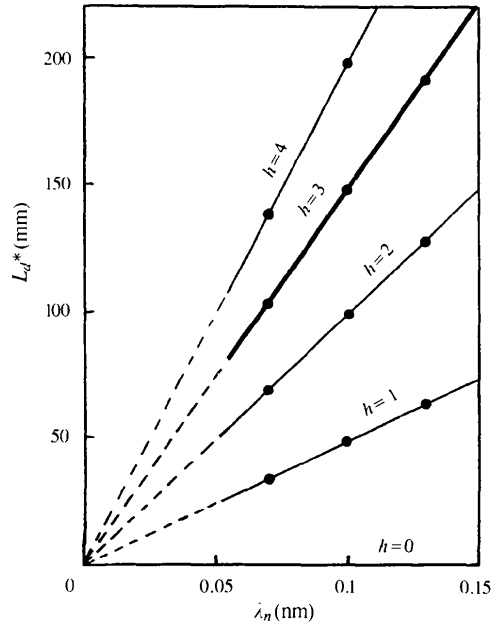

Figure 5
Optimum gap distance L_d* *versus* the wavelength λ_n obtained from Fig. 4.

3. Discussion

In the case of a narrow emittance electron beam of several nm rad, the beam size is approximately 0.2 mm or less. It is therefore very important to run the beam straight in a very long undulator so as to make the beam overlap with the generated radiation in the whole length of the undulator. One method of aligning the beam is to steer the beam at each short undulator while subsequently turning the undulator on and off downstream and observing the radiation on the beam axis. It is then necessary to install steering permanent magnets between the undulators. In such a situation the gap distance between the undulators needs to be sufficiently wide to avoid mutual interaction of the fields of the undulators and steering magnets, which is caused by non-unit permeability of permanent magnets. In addition, the end correction of each undulator needs to be done well.

4. Conclusions

We have discussed the radiation spectrum of a very long undulator separated into a number of short ideal undulators with a constant gap distance between these sections in considering the numerical example of a 30 m-long undulator for SPring-8. It was shown that the peak height of the spectrum of such an undulator decreases as the gap distance increases, but not significantly as long as the distance is less than 5 mm or so in the present example, while the spectrum width is kept almost constant. It was also shown that the peak height and width of the spectrum do not deteriorate if the radiation phases of different undulators are matched by dispersive sections between them.

APPENDIX
Transit time of an electron in a three-pole wiggler

Suppose an electron passes through a three-pole wiggler with a length L_w, then the orbit of the electron trajectory in the wiggler is given by

$$L_e = \int_0^{L_d} [1 + (\mathrm{d}x/\mathrm{d}z)^2]^{1/2}\,\mathrm{d}z, \quad (25a)$$

$$\mathrm{d}x/\mathrm{d}z = (ce/E)\int_0^z B(u)\,\mathrm{d}u, \quad (25b)$$

where $x(z)$ is the transverse position of the electron. Assuming, for simplicity, constant peak fields $-B_p$, B_p and $-B_p$ for the lengths $L_w/4$, $L_w/2$ and $L_w/4$, respectively,

in the wiggler, we obtain

$$L_e = L_w(1 + D/\gamma^2) \tag{26a}$$

$$D \simeq (1/96)(e/mc)^2(B_p/L_w)^2 = 3600(B_pL_w)^2. \tag{26b}$$

The transit time of the electron over the wiggler is

$$\tau_e = (L_w/c)[1 + (1 + 2D)/2\gamma^2]. \tag{27}$$

Accordingly, the transit-time difference between the electron and electromagnetic wave over the wiggler is

$$\Delta t_w = (L_w/c)(1 + 2D)/2\gamma^2. \tag{28}$$

References

Chavanne, J., Chinchio, E., Diot, M., Elleaume, P., Frachon, D., Marechal, X., Mariaggi, C. & Revol, F. (1992). *Rev. Sci. Instrum.* **63**, 317–320.

Diviacco, B. & Walker, R. P. (1993). *Proc. Part. Accel. Conf.* pp. 1593–1595. Piscataway, NJ: IEEE.

Elleaume, P. (1983). *J. Phys. (Paris) Colloq.* **44**, 333–350.

Hara, M., Be, S. H., Kamitsubo, H., Kumagai, N., Motonaga, S., Nagaoka, R., Oikawa, Y., Sasaki, S., Takebe, H., Takeshita, I., Tanaka, H. & Wada, T. (1990). *Proc. 2nd Eur. Part. Accel. Conf.* pp. 466–468. Gif-sur-Yvette: Editions Fontières.

Moriguchi, S., Udagawa, K. & Ichimatsu, S. (1972). *Mathematical Formula II*, p. 17. Japan: Iwanami Press.

Yamamoto, Y., Shioya, T., Kitamura, H. & Tsuchiya, K. (1995). *Rev. Sci. Instrum.* **66**, 1996–1998.